# High-pressure photodissociation of water as a tool for hydrogen synthesis and fundamental chemistry

**Matteo Ceppatelli, Roberto Bini[1], and Vincenzo Schettino**

European Laboratory for Non-Linear Spectroscopy, Via N. Carrara 1, I-50019 Sesto Fiorentino, Florence, Italy; and Dipartimento di Chimica, Universitá di Firenze, Via della Lastruccia 3, I-50019 Sesto Fiorentino, Florence, Italy

**High-pressure methods have been demonstrated to be efficient in providing new routes for the synthesis of materials of technological interest. In several molecular compounds, the drastic pressure conditions required for spontaneous transformations have been lowered to the kilobar range by photoactivation of the reactions. At these pressures, the syntheses are accessible to large-volume applications and are of interest to bioscience, space, and environmental chemistry. Here, we show that the short-lived hydroxyl radicals, produced in the photodissociation of water molecules by near-UV radiation at room temperature and pressures of a few tenths of a gigapascal (GPa), can be successfully used to trigger chemical reactions in mixtures of water with carbon monoxide or nitrogen. The detection of molecular hydrogen among the reaction products is of particular relevance. Besides the implications in fundamental chemistry, the mild pressure and irradiation conditions, the efficiency of the process, and the nature of the reactant and product molecules suggest applications in synthesis.**

high-pressure chemistry | photocatalysis

T he application to molecular systems of suitable external pressures causes a density increase that determines a strengthening of the intermolecular interactions leading first to changes in the aggregation state of the material, and then to crystalline phase transitions (1). Upon further compression, the possible overlap of the electronic density of nearest-neighbor molecules can also trigger a complete reconstruction of the chemical bonds, giving rise to new materials in some cases recoverable at ambient conditions (2). After the pioneering work on the pressure-induced polymerization of cyanogen (3) and acetylene (4) crystals, several simple molecular crystals have been reported to react upon application of suitable external pressure, giving rise to high-quality polymeric (5–7) and amorphous (8–10) materials of potential technological interest. These transformations require pressures from several to 100 GPa, as in the nitrogen case (7), but the reaction threshold pressure has been successfully lowered in almost all of the unsaturated hydrocarbons studied so far by a photoactivation of the high-pressure reactions (11). In some cases, an increasing selectivity (5) or the opening of new reaction paths (12) is also observed. These syntheses are appealing because only physical methods are used, thus representing an interesting perspective for a green chemistry (13).

The mechanisms governing the photoinduced reactivity of molecular systems derive from the structural and charge density distribution changes after an electronic transition. In general, the excited molecule is characterized by a reduced binding order that determines molecular bonds stretching, a lowering of rotational and torsional barriers, an increase in the polarity, and even dissociation and ionization. These species can be particularly aggressive from a chemical point of view and, depending on their lifetime and free mean path, can trigger and propagate a reaction (14). It is therefore evident that these reactions become more and more relevant with increasing pressure because the increasing density of the materials results in reduced intermolecular distances that favor the interaction between excited and ground-state molecules. The efficiency of these processes is also attested to by several reactions occurring in pure condensed unsaturated

hydrocarbons triggered by 2-photon (TP) excitations realized with cw (continuous wave) low-power laser sources that, because of the small cross-section of TP transitions, ensure catalytic amounts of excited species (5, 6, 12, 15).

Among simple molecular systems, water is of primary importance because of its abundance on the Earth's surface and because it is the most abundant polyatomic molecule in the visible universe (16). In addition, chemical reactions taking place in liquid water are essential for many processes in environmental science and biology. The photodissociation of water is the principal step in many chemical reactions occurring in the Earth's atmosphere, in planets, comets, or other space environments. Absorption of vacuum UV (VUV) photons can give rise to single and multiple ionization with the formation of neutral and ionic fragments, either in the ground or in the excited states, able to trigger many chemical reactions.

Photoreactions in gas mixtures containing CO, $CO_2$, $CH_4$, $NH_3$, $N_2$, and $H_2O$ [components of the primitive Earth atmosphere (17, 18)] have been studied to investigate the photochemical abiotic formation of bioorganic compounds (19). The high-energy photons ($\lambda < 185$ nm) used in these experiments should simulate the solar irradiation in planetary or primitive Earth environments. The choice of these drastic irradiation conditions is dictated by the energies required to excite, and eventually dissociate, these simple molecules. More than 10.5 eV (118 nm) is necessary to dissociate at ambient pressure the triple bonds of $N_2$ and CO for the generation of the precursors of bioorganic compounds (20). Slightly lower energies are required for photogeneration of OH and H radicals from water molecules. For instance, evidence for radical formation has been reported in 1-photon (184.9 nm) absorption experiments (21). Photolysis at 184.9 nm in low-pressure gaseous $CO/H_2O$ mixtures has been used to explain the presence of methane in the Martian atmosphere (22). Mixed ices containing $H_2O$ and CO (23) or $C_2H_2$ (24) irradiated at 10 K with wavelengths <120 nm produce small amounts of $CH_3OH$, $H_2CO$, and $CO_2$, in addition to some CO and $CH_4$ in the case of $C_2H_2$.

Despite these important results, studies employing lower-energy photons, where the solar radiation is peaked, are almost missing. Two-photon absorption experiments (281–286 nm) have shown the formation of OH and H radicals (25), suggesting the possibility of using lower-energy photons to generate radicals through multiphoton absorption processes. In this respect, the high-pressure photodissociation of water is of particular relevance because it could occur with much lower irradiation energies because of the red shift of the electronic transitions with pressure, whereas the higher density could increase the efficiency of the OH and H radicals as reaction initiators. The irradiation of water under high pressure is an almost unexplored topic despite the fact that these conditions are encountered in

**Fig. 1.** Photomicrographs illustrating the history of the N₂/H₂O mixture. (1) The sample at 0.6 GPa after the loading. The Raman spectra clearly show that the *b* region is mainly fluid nitrogen, whereas the solid fraction *a* is the nitrogen clathrate hydrate (28). (2) At 0.1 GPa after the clathrate decomposition and before the irradiation cycles. The *c* region is essentially composed of water. (3) After 3 h of irradiation with 500 mW of the 350-nm line focused to irradiate all of the sample (150 $\mu$m in diameter). (4) After 5 additional hours of irradiation with 200 mW focused in the nitrogen-rich region to a spot of 40 $\mu$m to increase the power density by a factor 6 with respect to the previous irradiation cycle.



**Fig. 2.** Raman spectra of the N₂/H₂O mixture at 0.1 GPa. (Line a) Spectrum measured before irradiation in the nitrogen-rich region (see Fig. 1(2)). (Line b) Spectrum measured in the water-rich region after 3 h of irradiation with 500 mW of the 350-nm line focused to irradiate all of the sample (150 $\mu$m in diameter), the 2 strong bands just >1,000 cm$^{-1}$ are the $R_2$ and $R_1$ ruby fluorescence lines. (Line c) Spectrum measured in the nitrogen-rich region (same conditions as line b). (Line d) Spectrum measured in the nitrogen-rich region after 5 additional hours of irradiation with 200 mW of the 350-nm line focused to 40 $\mu$m to increase the power density by a factor 6. (Line e) Reference spectrum of a H₂/Ar mixture (5% H₂ molar fraction) at 1.4 GPa.

nature and have been invoked (catastrophic meteoritic events) as possible causes of the origin of life on Earth (26). Cleavage of the water molecule with the formation of an O₂–H₂ alloy is reported >2.5 GPa in ice by using X-ray photons ($\approx$10 keV) (27).

Here, we report experiments in which we successfully used near-UV radiation (350 nm) to dissociate water molecules at moderate pressures through TP absorption processes. The generated OH and H radicals trigger the reaction in a nitrogen/water fluid mixture and in a carbon monoxide clathrate hydrate.

## Results

**N₂/H₂O Mixture.** After loading, at pressure <1 GPa, the N₂/H₂O mixture appears as a 2-phase heterogeneous system (see Fig. 1). Raman spectra could be measured with a spatial resolution of $\approx$5 $\mu$m, thus allowing the in situ characterization of the material. The fluid phase is essentially composed of pure nitrogen because only the band relative to the N–N stretching mode is detected. In contrast, the solid phase presents a doublet in the same region of the Raman spectrum, allowing for its identification as a nitrogen clathrate hydrate crystal (28). The sample is irradiated for 1 h, between 0.6 and 0.9 GPa, by using 500 mW of the 350-nm Ar$^+$ laser line focused to a spot of $\approx$150 $\mu$m in diameter to match the sample dimension. Neither changes in the sample appear-

ance nor new bands in the Raman spectra are detected after the irradiation, thus indicating the chemical stability of the clathrate under these conditions. The clathrate is reported to be stable at ambient temperature down to 0.14 Gpa, where it decomposes (29). The pressure is lowered down to 0.1 GPa observing the clathrate decomposition and the obtainment of a 2-fluid phase system. The Raman spectra indicate that the smaller phase of the sample (labeled c in Fig. 1) is essentially composed of water, whereas the largest one is composed of nitrogen. A new homogeneous irradiation (500 mW, 3 h) of all of the fluid sample gives rise to remarkable changes in the sample appearance: Some bubbles form in the nitrogen-rich region, whereas the extension of the water region reduces. Samples of pure water or nitrogen are also irradiated under the same *P-T-h$\nu$* conditions, but no changes are detected either by visual observation or by the Raman spectra.

In Fig. 2 we report the Raman spectra measured after each irradiation cycle performed at 0.1 GPa in the fluid sample. The spectrum measured in the water-rich region presents only 3 new peaks between 2,080 and 2,160 cm$^{-1}$, likely ascribable to the nitrogen stretching of N₂–H₂O complexes. Evidence of a chemical reaction is gained by the analysis of the bubbles. New sharp peaks are observed at 589, 871, and 940 cm$^{-1}$, whereas a broad band of variable intensity and frequency depending on the sample region is observed between 1,550 and 1,580 cm$^{-1}$. After a new irradiation cycle of 5 h, performed in the nitrogen rich phase by focusing 200 mW to a spot of 40 $\mu$m in diameter to increase the power density by approximately a factor 6, the intensity of the 589 cm$^{-1}$ band increases, and new peaks are detected at 358, 815, 895, and 1,465 cm$^{-1}$. The intensity of the broad band at 1,550 cm$^{-1}$ is, in contrast, considerably reduced.

The 3 low-frequency bands (358, 589, and 815 cm$^{-1}$) are easily identified as the $S_0(0)$, $S_0(1)$, and $S_0(2)$ rotational bands of H₂ (30). The comparison with a compressed H₂/Ar mixture (top spectrum of Fig. 2) confirms this assignment. The band at 1,465 cm$^{-1}$ can be confidently assigned to the N═O stretching of
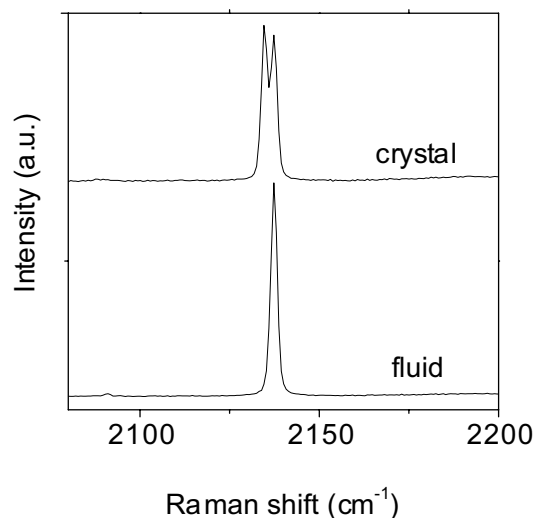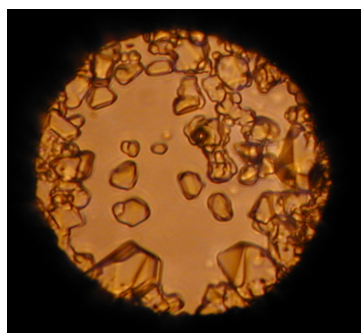
**Fig. 3.** Raman characterization of the CO/H$_2$O mixture. The photomicrograph illustrates the CO/H$_2$O mixture at 0.6 GPa after the loading. The Raman spectrum of the fluid phase shows that it is mainly composed of CO. The spectrum of the solid fraction presents a doublet as observed in the nitrogen clathrate hydrate (28), thus allowing its identification as a carbon monoxide clathrate hydrate.

nitrosoamines (N—N═O) or to the N═N stretching of dimeric nitroso or azoxy compounds (N═N → O). Nitroso compounds could also account for the 895 cm$^{-1}$ band (N—N stretching), but also the N—O stretching mode of N—OH groups and the O—O stretching of peroxides give a strong Raman band close to this frequency at 900 cm$^{-1}$ and 880 cm$^{-1}$ (in H$_2$O$_2$), respectively. The broad band between 1,550 and 1,580 cm$^{-1}$ is probably due to the superposition of vibrational modes of different species: Raman peaks associated with the stretching modes of O$_2$, —N═N— and nitro (N—NO$_2$) groups are expected in this frequency range. Products such as azides, nitrates, nitrites, and all of the simplest nitrogen oxides (NO, N$_2$O, N$_2$O$_4$, and N$_2$O$_3$) can be confidently ruled out on the basis of the Raman results.

After the last irradiation, the sample is monitored for several hours by measuring the Raman spectrum of different regions without observing any change in the reaction products composition. Also, the pictures collected show a sample appearance unchanged with respect to the conclusion of the irradiation. Therefore, we can conclude that the chemical species formed under irradiation do not further react or transform back to the reactants.

**CO/H$_2$O Mixture.** As for N$_2$/H$_2$O, the samples of CO/H$_2$O mixtures appear inhomogeneous after the loading. Crystals of variable dimensions coexist with a homogeneous transparent region formed by fluid CO (see Fig. 3). The crystalline fraction presents a Raman spectrum characterized by a doublet in the fundamental CO stretching region. This spectrum closely resembles that

reported in Fig. 1 for the N$_2$/H$_2$O mixture and assigned to the clathrate hydrate (28). In analogy with the nitrogen case, and considering that both the components of the mixture should be fluid at these *P-T* conditions, we can confidently assign this spectrum to the CO clathrate hydrate. The formation of carbon monoxide clathrate hydrate is reported to take place more easily than the nitrogen clathrate hydrate (31), but its stability conditions are known only at ambient pressure (32). In contrast to the observation for the N$_2$/H$_2$O mixtures, the reactivity of the CO/H$_2$O mixture under irradiation is observed also in the clathrate hydrate crystal. For this reason, all of the different experiments have been performed between 0.4 and 0.6 GPa in the heterogeneous phase.

Compressed CO is reported to react at quite low pressure especially under irradiation (33). To understand the role of water in the reaction, we have performed different experiments to distinguish the reactivity of pure CO from that of the CO/H$_2$O mixture and to separate the effect of pressure from that of laser irradiation (Fig. 4). FTIR spectra reveal the formation of a very small amount of CO$_2$ in the mixture left for >80 h at ≈0.5 Gpa, avoiding any irradiation of the sample. The amount of CO$_2$ is considerably larger when pure CO is exposed at the same pressure for 3 h to 100 mW of the 350-nm laser line focused to a 150-$\mu$m diameter focal spot, despite the fact that it is reported to react under irradiation at ambient temperature only for T >3.5 GPa (33). No bubbles form in the sample after the irradiation, but traces of a brownish solid product are observed. In contrast, dramatic changes in the sample aspect take place when the CO/H$_2$O mixture is irradiated under the same conditions of pure CO, clearly evidencing the active role of water in the photoinduced reactivity. Several bubbles are observed in the transparent region of the reacted sample that also presents a large area covered by a brownish solid material (see Fig. 5). A much larger amount of CO$_2$ is produced during the irradiation, whereas the water progressively disappears. In fact, the characteristic water broad bands (≈800, 1,600, and 3,250 cm$^{-1}$) almost vanish after 8 h of irradiation (see Fig. 4).

The Raman spectra measured after these irradiation cycles show a very strong fluorescence background, due to the dark solid product, that prevents the detection of any product band but the CO$_2$ $\nu^+$ peak, the high-frequency component of the Fermi resonance doublet $\nu_1;2\nu_2$ at 1,360 cm$^{-1}$. For this reason, we have performed shorter cycles (10–30 min), under the same irradiation conditions, measuring after each cycle the Raman spectrum of the bubbles that are the major components of the transparent regions. With this approach, after a few minutes of irradiation, we are able to detect, besides CO$_2$, also the formation of H$_2$, revealed by the appearance of the 4 Raman rotational bands (S$_0$(0)-S$_0$(3)), whereas the CO band (stretching mode) at 2,135 cm$^{-1}$ simultaneously decreases (see Fig. 5).

The dark material formed during the reaction is recovered at ambient pressure, and some hints about its composition can be derived from the IR spectrum reported in Fig. 6. The spectrum is quite similar to that measured in ref. 33 on the material recovered by the pressure induced reaction of pure CO and then exposed to the atmosphere. Remarkable here is the intensity of the bands relative to C—H bending and stretching modes.

## Discussion

Both the N$_2$/H$_2$O and CO/H$_2$O compressed mixtures exhibit a remarkable reactivity under irradiation with the 350-nm laser line. In contrast, the pure components are stable (N$_2$ and H$_2$O) or show a moderate instability (CO) under the same *P-T-h$\nu$* conditions. These results indicate the active role of water in triggering the photochemical reaction. The absorption spectrum of water has been recently measured between 6.0 and 11.0 eV by synchrotron radiation (34). Three absorption bands centered at 7.447, 9.672, and 10.011 eV have been assigned to the transitions from the X̃ ($^1A_1$) lowest neutral ground state to the Ã ($^1B_1$), B̃
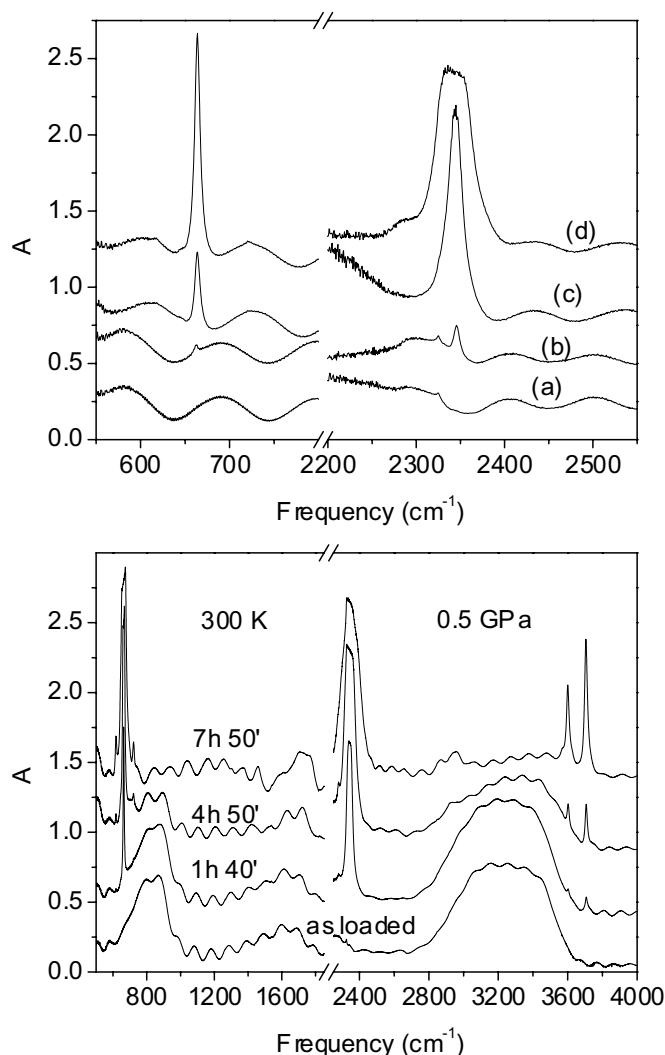
**Fig. 4.** Monitoring the reaction of the CO/H₂O mixture by FTIR spectra. (*Upper*) CO₂ bending (*Left*) and antisymmetric stretching (*Right*) regions measured at 0.5 GPa immediately after the loading of the mixture (line a); after the mixture has been kept 64 h at 0.45 GPa and 21 h at 0.65 Gpa (line b); in pure CO after 3 h irradiation with 100 mW of the 350-nm line (line c); in the mixture after irradiation in the same conditions as line c (line d). (*Lower*) Evolution of the IR spectrum of the CO/H₂O mixture as a function of the irradiation time. The spectra are measured after irradiation with 100 mW of the 350-nm line for the reported duration.



**Fig. 5.** Photomicrographs and Raman spectra illustrating the history of the CO/H₂O mixture. (1) The sample at 0.4 GPa before irradiation. The a region is essentially fluid CO, whereas the solid fraction b is the clathrate hydrate (see Fig. 3). (2) The sample at the same pressure after 1 h 25 min of irradiation with 100 mW of the 350-nm line. The dark region is a recoverable solid product, and the Raman spectra measured in this sample region exhibit a strong fluorescence background. Molecular hydrogen and carbon dioxide are detected in the bubbles region. (3 and 4) (Line a) Spectrum measured at 0.4 GPa immediately after the loading. (Line b) Spectrum measured at the same pressure after 20 min of irradiation with 100 mW of the 350-nm line. (Line c) Reference spectrum of a H₂/Ar mixture (5% H₂ molar fraction) at 1.4 GPa.

($^1A_1$), and $\tilde{C}$ ($^1B_1$) states, respectively. A fourth band centered at 10.163 eV is due to excitation to the $\tilde{D}$ ($^1A_1$) state. The ionization energy threshold of H₂O is reported >12 eV (see ref. 34 and references therein). The first absorption band is quite broad, with the electronic origin located at 7.069 eV. The lowest excited state, $\tilde{A}$ ($^1B_1$), has been shown to be dissociative like all of the other excited states of water. The direct excitation to this state (155–175 nm) gives rise to a dissociation proceeding on a single potential-energy surface and producing a hydrogen atom and a hydroxyl radical in its electronic ground state ($X^2\Pi$) with little internal excitation (35). Excitation with lower-wavelength radiation gives access to higher-energy states, like the $\tilde{B}(^1A_1)$ state, and the dissociation can proceed through the potential-energy surfaces relative to both the $\tilde{A}$ and the ground $\tilde{X}$ states. Conical intersections drive these processes to collinear H—O—H and O—H—H molecular geometries (see ref. 36 and references therein).

In our experiments, the employment of the 350-nm laser line causes the excitation of the lowest electronic excited state

through the symmetry allowed $\tilde{X}$ ($^1A_1$) → $\tilde{A}$ ($^1B_1$) 2-photon transition. The catalytic amounts of hydroxyl radicals produced in this process are able to trigger the reactions in the mixtures. Despite the impossibility of depicting a precise reaction evolution, all of the products identified from the reaction in the N₂/H₂O mixtures suggest the attack of the nitrogen molecule by the OH radical, identified as the active species also in low-temperature photoreactions of mixed ices (37) and point to the incomplete cleavage of the N—N bond. This latter observation agrees with the results of VUV photolysis (121.6 nm) studies of ices containing molecular N₂. These photoreactions appeared indeed inefficient at breaking the N—N bonds (38). At least in the N₂/H₂O mixture, the hydrogen atoms seem mainly to recombine to give molecular hydrogen. Much more complex is the interpretation of the reaction in the CO/H₂O mixture, where the instability of CO can play an active role in the reaction. Despite the considerable amount of hydrogen incorporated by the recoverable solid product
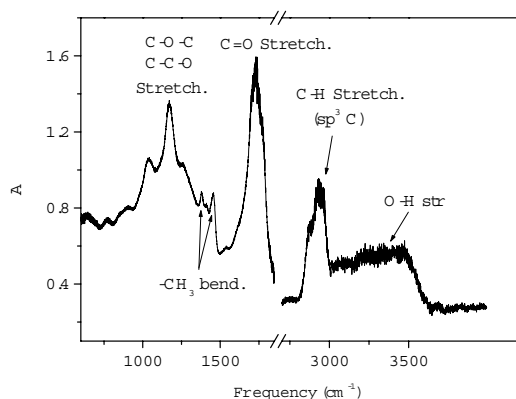
**Fig. 6.** IR spectrum of the recovered solid material from the CO/H₂O reaction. The spectrum has been measured after the complete release of the pressure. An assignment of the most significant absorption bands is also reported.

as C—H and O—H bonds, the straightforward obtainment of molecular hydrogen after very short irradiation cycles points to a massive participation of water in the reaction.

In conclusion, the present results highlight the role of water as a powerful high-pressure photoactivated reactant and radical initiator able to trigger chemical reactions even with very stable molecules like nitrogen. High pressure, through a fine and effective tuning of intermolecular distances, permits the activation of the reaction at ambient temperature with near-UV photons. Water quantitatively transforms during these processes, and, among the reaction products, the synthesis of hydrogen is highly relevant. Hydrogen has been considered the energy vector of the future, but at present, ≈95% of the hydrogen production comes from nonrenewable sources such as natural gas, oil, and coal, thereby making alternative synthetic methods and hydrogen-renewable sources in great demand (39). The mild pressure

and irradiation conditions used in this work suggest an eventual route to the synthesis of molecular hydrogen from compressed water-enriched air. In fact, the pressure and temperature conditions in which the reaction occurs are currently used in industrial reactors, making feasible, from a technical point of view, the extension of this synthetic method to large-volume apparatuses.

## Methods

A membrane diamond anvil cell (MDAC) equipped with IIa-type diamonds was used to pressurize the mixtures. A rhenium gasket of ≈150 $\mu$m in diameter and 45 $\mu$m in thickness was used to contain the samples. The mixtures were loaded by separately condensing H₂O and CO or N₂ (≥99.99%) onto the diamonds while the cell was mounted on the cold tip of a close-cycle cryostat. The deposition was realized through a capillary, placed at ≈2 mm from the diamond's surface, connected through a flange to a deposition line that was pumped several hours before starting the cooling of the cell. Water was condensed at T <120 K by using helium as gas carrier. CO or N₂ were then condensed when the temperature reached ≈30 K. The deposition steps could be visually followed by observation through a microscope, and the relative amounts could be roughly adjusted. Once the sample region was completely covered by the crystalline sample, the cell was screwed and helium pressure applied in the membrane to seal the sample. The temperature was then raised by keeping the membrane pressure constant. Infrared and Raman spectra were used to check the sample purity. The pressure was measured by the ruby fluorescence method. The high-pressure reactions were triggered by focusing the UV multiline emission of an Ar ion laser (350 nm) onto the sample with power ranging from 50 to 610 mW, taking care to homogeneously irradiate the whole sample. FTIR absorption measurements were performed with a Bruker-IFS 120 HR spectrometer modified for high-pressure measurements (40, 41). The instrumental resolution was 1 cm⁻¹. Raman spectra were measured in a back-scattering geometry by using 40–250 mW of the 647.1-nm line of a Kr⁺ laser. The scattered light was dispersed by a single-stage monochromator (900 grooves per millimeter) and analyzed by a CCD detector with a resulting instrumental resolution of 0.7 cm⁻¹.

1. Hemley RJ (2000) Effects of high pressure on molecules. *Annu Rev Phys Chem* 51:763–800.
2. Schettino V, Bini R, Ceppatelli M, Ciabini L, Citroni M (2005) Chemical reactions at very high pressure. *Adv Chem Phys* 131:105–242.
3. Yoo CS, Nicol M (1986) Kinetics of a pressure-induced polymerization reaction of cyanogen. *J Phys Chem* 90:6732–6736.
4. Aoki K, et al. (1988) Raman study of the solid-state polymerization of acetylene at high pressure. *J Chem Phys* 89:529–534.
5. Citroni M, Ceppatelli M, Bini R, Schettino V (2002) Laser-induced selectivity for dimerization versus polymerization of butadiene under pressure. *Science* 295:2058–2060.
6. Chelazzi D, Ceppatelli M, Santoro M, Bini R, Schettino V (2004) High-pressure synthesis of crystalline polyethylene using optical catalysis. *Nat Mater* 3:470–475.
7. Eremets MI, Gavriliuk AG, Trojan IA, Dzivenko DA, Boehler R (2004) Single-bonded cubic form of nitrogen. *Nat Mater* 3:558–563.
8. Iota V, Yoo CS, Cynn H (1999) Quartzlike carbon dioxide: An optically nonlinear extended solid at high pressures and temperatures. *Science* 283:1510–1513.
9. Santoro M, et al. (2006) Amorphous silica-like carbon dioxide. *Nature* 441:857–860.
10. Ciabini L, et al. (2007) Triggering dynamics of the high-pressure benzene amorphization. *Nat Mater* 6:39–43.
11. Bini R (2004) Laser-assisted high-pressure chemical reactions. *Acc Chem Res* 37:95–101.
12. Citroni M, Ceppatelli M, Bini R, Schettino V (2007) Dimerization and polymerization of isoprene at high pressures. *J Phys Chem B* 111:3910–3917.
13. Anastas P, Warner J (1998) *Green Chemistry: Theory and Practice* (Oxford Univ Press, New York).
14. Citroni M, Bini R, Foggi P, Schettino V (2008) The role of excited electronic states in the high-pressure amorphization of benzene. *Proc Natl Acad Sci* 105:7658–7663.
15. Ciabini L, Santoro M, Bini R, Schettino V (2002) High pressure photoinduced ring opening of benzene. *Phys Rev Lett* 88:085505.
16. Nisini B (2000) Astronomy—Water's role in making stars. *Science* 290:1513–1514.
17. Kramers JD (2003) Volatile element abundance patterns and an early liquid water ocean on Earth. *Precamb Res* 126:379–394.
18. Kasting JF (1990) Bolide impacts and the oxidation state of carbon in the Earth's early atmosphere. *Origins Life Evol Biosphere* 20:199–231.
19. Miller SL, Urey HC (1959) Organic compound synthesis on the primitive Earth: Several questions about the origin of life have been answered, but much remains to be studied. *Science* 130:245–251.
20. Takahashi J, et al. (2005) Photochemical abiotic synthesis of amino-acid precursors from simulated planetary atmospheres by vacuum ultraviolet light. *J Appl Phys* 98:024907.
21. Sokolov U, Stein G (1966) Photolysis of liquid water at 1849 Å. *J Chem Phys* 44:3329–3337.
22. Bar-Nun A, Dimitrov V (2006) Methane on Mars: A product of H₂O photolysis in the presence of CO. *Icarus* 181:320–322.
23. Watanabe N, Nagaoka A, Shiraki T, Kouchi A (2004) Hydrogenation of CO on pure solid CO and CO–H₂O mixed ice. *Astrophys J* 616:638–642.
24. Wu CYR, et al. (2002) Extreme ultraviolet photon-induced chemical reactions in the C₂H₂–H₂O mixed ices at 10 K. *Icarus* 156:456–473.
25. Wang CC, Davis LI, Jr (1974) Two-photon dissociation of water: A new OH source for spectroscopic studies. *J Chem Phys* 62:53–55.
26. Daniel I, Oger P, Winter R (2006) Origins of life and biochemistry under high-pressure conditions. *Chem Soc Rev* 35:858–875.
27. Mao WL, et al. (2006) X-ray-induced dissociation of H₂O and formation of an O₂-H₂ alloy at high pressure. *Science* 314:636–638.
28. van Hinsberg MGE, Scheerboom MIM, Schouten JA (1993) The vibrational-spectra of N₂ in clathrate-hydrates—A new high-pressure phase-transition. *J Chem Phys* 99:752–754.
29. Sasaki S, Hori S, Kume T, Shimizu H (2003) Microscopic observation and in situ Raman scattering studies on high-pressure phase transformations of a synthetic nitrogen hydrate. *J Chem Phys* 118:7892–7897.
30. Ulivi L, Zoppi M, Gioè L, Pratesi G (1998) Molecular hydrogen internuclear distance in high-pressure fluid and solid phases at room temperature. *Phys Rev B* 58:2383–2386.
31. Iro N, Gautier D, Hersant F, Bockelée-Morvan D, Lunine JI (2003) An interpretation of the nitrogen deficiency in comets. *Icarus* 161:511–532.
32. Mohammadi AH, Anderson R, Tohidi BI (2005) Carbon monoxide clathrate hydrates: Equilibrium and thermodynamic modeling. *Am Inst Chem Eng J* 51:2825–2833.
33. Evans WJ, et al. (2006) Pressure-induced polymerization of carbon monoxide: Disproportionation and synthesis of an energetic lactonic polymer. *Chem Mater* 18:2520–2531.
34. Mota R, et al. (2005) Water VUV electronic state spectroscopy by synchrotron radiation. *Chem Phys Lett* 416:152–159.
35. Andresen P, Schinke R (1987) in *Molecular Photodissociation Dynamics*, eds Ashfold MNR, Baggott JE (Royal Society of Chemistry, London), Chap 3.

36. Harich SA, et al. (2000) Photodissociation of $H_2O$ at 121.6 nm: A state-to-state dynamical picture. *J Chem Phys* 113:10073–10090.
37. Watanabe N, Kouchi A (2002) Measurements of conversion rates of CO to $CO_2$ in ultraviolet-induced reaction of amorphous $D_2O(H_2O)$/CO amorphous ice. *Astrophys J* 567:651–655.
38. Elsila J, Allamandola LJ, Sandford SA (1997) The 2140 $cm^{-1}$ (4.673 microns) solid CO band: The case for interstellar $O_2$ and $N_2$ and the photochemistry of nonpolar interstellar ice analogs. *Astrophys J* 479:818–838.
39. National Research Council and National Academy of Engineering of the National Academies (2004) *The Hydrogen Economy Opportunities, Costs, Barriers, and R&D Needs* (National Academies Press, Washington, DC).
40. Bini R, Ballerini R, Pratesi G, Jodl HJ (1997) Experimental setup for Fourier transform infrared spectroscopy studies in condensed matter at high pressure and low temperatures. *Rev Sci Instrum* 68:3154–3160.
41. Gorelli FA, Santoro M, Ulivi L, Bini R (1999) The epsilon phase of solid oxygen: Evidence of an $O_4$ molecule lattice. *Phys Rev Lett* 83:4093–4096.

CHEMISTRY